Thermotropic and Chiroptical Properties of Poly{(+)-2,5-bis[4-((*S*)-2-methylbutoxy)phenyl]styrene} and Its Random Copolymer with Polystyrene

Anhua Liu, Junge Zhi, Jiaxi Cui, Xinhua Wan,* and Qifeng Zhou*

Beijing National Laboratory for Molecular Sciences, Key Laboratory of Polymer Chemistry and Physics of MOE, College of Chemistry and Molecular Engineering, Peking University, Beijing 100871, China

Received May 21, 2007; Revised Manuscript Received July 9, 2007

ABSTRACT: Poly{(+)-2,5-bis[4-((*S*)-2-methylbutoxy)phenyl]styrene} (PMBPS) and its random copolymers with polystyrene were synthesized via atom transfer radical polymerization and conventional radical copolymerization, respectively. The dependences of thermotropic and chiroptical properties on the degrees of polymerization (DPs) of homopolymers and on the compositions of copolymers were investigated to correlate the liquid crystallinity and helical chain structure of PMBPS. When DP < 53, PMBPS revealed no mesophase; when 53 < DP < 80, the polymer formed columnar nematic (Φ_N) phase; whereas, when DP ≥ 80, hexatic columnar nematic (Φ_{HN}) phase was generated. The monomer MBPS displayed positive optical rotation, while the oligomers and polymers showed negative optical rotations. The strength intensified with DP and leveled off at DP = 53, suggesting a stable helix started. The random nature of copolymers was indicated by the reactivity ratios of two monomers ($r_{MBPS} = 0.67$, $r_{St} = 0.98$), and further supported by smooth variation of single glass transition temperature. When the feed molar fraction of MBPS (x) was less than 59%, the optical rotations of copolymers were positive and scaled linearly with the proportion of chiral monomer, implying no new chiral structure developed. When x > 59%, the optical rotations decreased with increasing MBPS content and finally became negative when x reached above 90%, suggesting the MBPS segment was long enough to develop a dominating helical structure with negative optical rotation. Among all the copolymers, only one with x value of as high as 99% could achieve mesophase (Φ_N). It was considered that a long enough helical structure, which acted as cylindrical building blocks, was the origin of PMBPS to form a liquid crystalline phase.

Introduction

One long-standing goal in liquid crystalline polymers (LCPs) is to understand structure−property relationship, which has attracted wide attention from both theoretical and practical viewpoints.[1] LCPs with mesogens located in the side groups are named as side-chain LCPs (SC-LCPs).[2] In terms of the way in which mesogens are linked to the polymer backbones, SC-LCPs can be categorized into either "side-end-fixed" or "side-on-fixed" type.[3−5] The former has mesogens linked at the end position, while another has mesogens linked at the waist or mass center position. According to Finklemann and Ringsdorf,[6] in order for SC-LCPs to achieve a mesophase, flexible spacers are usually needed to decouple the interaction between main chains and side chains, which readily disturbs the ordered arrangements of mesogens. Theoretical and experimental results have shown that the backbones of "side-end-fixed" SC-LCPs prefer to take a strong oblate conformation due to the packing between layers in smectic phase and various oblate or prolate conformations in nematic phase depending on temperature or chemical structure.[7−10] For "side-on-fixed" SC-LCPs, however, the backbones tend to take prolate conformation on the direction of mesogens because of an enhanced "jacket effect" exerted by the laterally attached mesogens compared to conventional "side-end-fixed" SC-LCPs.[11,12] Hardouin and co-workers have systematically examined the remarkable effect of the length of flexible spacer and aliphatic extremity and the dilution of the mesogen content in a homologous copolymers on the prolate anisotropy of the polymer main-chain by SANS.[13−16] Side-chain LC polyacetylenes (PAs) are special since the mesogens are linked to conjugated rigid main chains through flexible spacers.[17,18] By a contrast, conventional SC-LCPs usually have flexible backbones. A higher chain stereoregularity of side-chain LC PAs leads to a lower packing order.[19,20] When the spacers are short, the rigid main chain and mesogens form sheetlike molecules, which act as building blocks to generate highly ordered frustrated smectic phase.[20] When the spacers are long enough, the interaction of rigid backbone and the mesogens are decoupled, resulting in better mesogenic order.[21]

For the last 20 years, we have been working on an unique "side-on-fixed" SC-LCPs, named mesogen-jacketed liquid crystal polymers (MJLCPs).[12,22−29] In these polymers, the mesogens are laterally attached to flexible polyethylene chain on every second carbon atom via no or only short spacers. The highly crowded bulky and rigid side groups around backbone force the polymer main chain to adopt extended conformation as in semirigid or rigid MC-LCPs.[30,31] As a result, although MJLCPs belong to SC-LCPs chemically, they display many thermotropic properties characterized by MC-LCPs, such as high glass transition temperature,[22,27] broad temperature range of mesophase,[22−29] long persistence length in good solvent,[32,33] and forming banded texture after mechanical shearing in LC state.[34] Investigations based on one-dimensional and two-dimensional wide-angle X-ray diffraction, along with polarized light optical microscopy and differential scanning calorimetry, show that the most popular phase structure achieved by MJLCPs is columnar nematic phase (Φ_N).[35] Higher ordered LC structures like hexatic columnar nematic (Φ_{HN}) phase and hexagonal columnar (Φ_H) phase, and smectic C phase have also been discovered in some systems.[36−38]

* To whom correspondence should be addressed. Telephone: 86-10-6275 4187. Fax: 86-10-6275 1708. E-mail: (X.W.) xhwan@pku.edu.cn; (Q.Z.) qfzhou@pku.edu.cn.

10.1021/ma071141p CCC: $37.00
Published on Web 10/13/2007

Chart 1. Chemical Structure of Poly{(+)-2,5-bis[4-((*S*)-2-methylbutoxy)phenyl]styrene} (PMBPS)

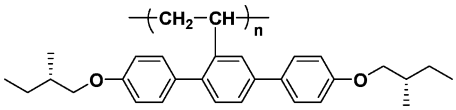

One interesting yet unsolved question related to MJLCPs is the nature of main-chain conformation (i.e., zigzag or helical) and how a conformation change caused by copolymerization with a non-mesogenic monomer exerts an influence on the mesomorphic property. When the concept of MJLCPs was first proposed in 1987,[12] it was speculated that the main chains of MJLCPs might adopt helical conformations due to the large steric hindrance of side groups, but no further evidence was provided. For the other polymers containing structurally rigid building blocks, Percec et al. found that the attachment of dendritic side groups to a flexible polymer backbone induced a helical conformation of the backbone by the self-assembly of its groups into a cylindrical structure.[39−43]

On the other side, copolymerization is one of the most commonly employed synthetic strategies to tuning the phase structures and transitions of both MC-LCPs and SC-LCPs.[44−48] For MJLCPs, however, the incorporation of non-mesogenic monomer into the polymer backbone would depress mesophase formation remarkably. For example, when 2,5-bis[(4-methoxyphenyl)oxycarbonyl]styrene (MPCS), one of the most often used monomers of MJLCPs, is copolymerized with styrene (St) and methyl methacrylate (MMA), liquid crystalline phase can only be obtained when the molar content of MPCS in copolymer exceeds 89% and 84%, respectively.[49] In a sharp contrast, although 2,5-di(*n*-butoxycarbonyl)styrene (BCS) cannot form mesophase by itself as St and MMA, when it is radically copolymerized with MPCS, all the resultant copolymers display stable mesophase under suitable conditions regardless of chemical compositions.[50] It is considered that St and MMA units cannot cooperate with MPCS to form extended conformation and act as constitutional disorders in polymer backbones. For BCS, however, since its homopolymer forms two-dimensional hexagonal columnar (Φ_H) phase,[36] it does not cause significant change in main chain conformation of PMPCS when being copolymerized with MPCS. However, it remains unknown why the chain conformations of MJLCPs are so sensitive to the introduction of non-mesogenic structural units.

Recently, we reported a novel optically active MJLCP, poly-{(+)-2,5-bis[4-((*S*)-2-methylbutoxy)phenyl]styrene} (PMBPS, Chart 1),[51] which consisted of a flexible polyethylene backbone substituted at every repeating units by latterly attached *p*-terphenyl derivatives via only one covalent bond. It was amazing that such an architecture led to an effective control over the secondary chiral structure in free radical polymerization even though the stereogenic chiral centers in the side chains were remote from main chain. The steric repulsion of bulky and highly crowded side groups restricted the rotations around the σ-bonds linking main chain carbons and gave rise to atropisomerism. And the calamitic *p*-terphenyl also served to help the long range chirality transfer from stereogenic centers in the side chains to the backbone. In addition, PMBPS is a sort of MJLCPs and possesses thermotropic liquid crystallinity, although the phase structure has not been identified yet.

Bearing in mind that a helical conformation might be responsible for the mesophase formation of MJLCPs, we think PMBPS is probably an idea system to study the correlation between the mesomorphic properties and the chiral secondary structures of MJLCPs since it is of either liquid crystallinity or helical conformation. Herein, we'll report on the synthesis and characterization of a series of MBPS homopolymers with varying molecular weights (MWs) and relatively narrow MW distributions via atom transfer radical polymerization, and the copolymers of MBPS and St (Chart 2) with various compositions via conventional radical copolymerization, separately. The dependences of thermotropic and chiroptical properties on the MWs of homopolymers and on the compositions of copolymers are explored by a combination of polarimetry, circular dichroism spectroscopy, differential scanning calorimetry, polarized light optical microscopy, and wide-angle X-ray diffractions to approach the relationship between the liquid crystallinity and helical structure of PMBPS. Although optical activity has been increasingly used for the study of conformational properties in synthetic polymers and their supramolecular states,[52−54] it is seldom employed to investigate the mechanism of mesophase formation of vinyl polymers like MJLCPs.

Chart 2. Chemical Structure of Poly{(+)-2,5-bis[4-((*S*)-2-methylbutoxy)phenyl]styrene}-*co*-polystyrene[a]

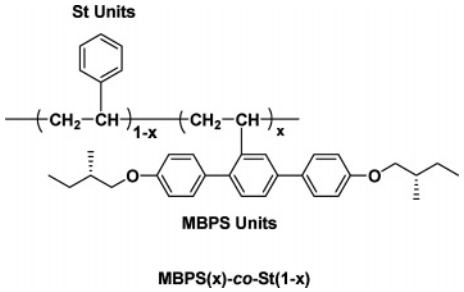

[a] The copolymer is abbreviated as MBPS(x)-*co*-St($1-x$), where x and $1-x$ denote the feed molar fractions of MBPS and St, respectively.

Experimental Section

Materials. *N*,*N*,*N*′,*N*′,*N*″-pentamethyldiethylenetriamine (PMDETA, 99%, Aldrich) and ethyl 2-bromo-2-methylpropanoate (EBMP, 99%, Aldrich) were used as purchased. Tetrahydrofuran (THF, Fisher Chemical Co., HPLC grade) was directly used in the gel permeation chromatography (GPC) and laser light scattering measurements. CuBr (98%, Aldrich) was purified by stirring overnight in acetic acid. After filtration, it was washed with ethanol and ether and then dried under vacuum. Styrene (St, Beijing Chemical Co., A.R.) was freed from the inhibitor via passing through a silica gel column. After drying over calcium hydride (Beijing Chemical Co., A.R.), it was distilled under vacuum. Benzoyl peroxide (BPO, Beijing Chemical Co., A.R.) was purified by recrystallization from ethanol. Anisole (Beijing Chemical Co., A.R.) was distilled out over CaH_2 just before use. THF (Beijing Chemical Co., A.R.) was distilled over CaH_2 to remove the reducing reagent for the use in circular dichroism (CD) and optical rotation measurements. The monomer MBPS was synthesized following the procedure reported previously.[51] Other reagents and solvents were purchased from Beijing Chemical Reagents Co. and used as received unless otherwise specified.

Atom Transfer Radical Polymerization (ATRP). MBPS homopolymers with different MWs were prepared via ATRP at 90 °C in anisole. The initiating system was EBMP/CuBr/PMDETA (1:1:1, molar ratio). The polymerization was allowed to continue for 24 h. The molecular weight was adjusted by changing the molar ratio of monomer to initiator. In a typical run, MBPS (1.00 g, 2.34 mmol), EBMP (0.03 g, 0.16 mmol), CuBr (0.02 mg, 0.16 mmol), PMDETA (0.03 mg, 0.16 mmol), and anisole (1.00 g) were introduced into a glass reaction tube. After three freeze−pump−thaw cycles, the tube was sealed under vacuum and put into an oil bath thermostated at 90 °C. The reaction was terminated after 24

Table 1. Atom Transfer Radical Polymerization of (+)-2,5-Bis[4-((*S*)-2-methylbutoxy)phenyl]styrene with Results and Properties of the Resultant Polymers

run[a]	convn (%)	$M_{n,GPC}$[c] (10^{-4})	PDI_{GPC}[c]	$M_{n,GPC-LS}$[d] (10^{-4})	DP[e]	PDI_{GPC-LS}[d]	$[\alpha]_{365}^{20}$ [f] (deg°)	T_g[g] (°C)	liquid crystallinity
P-1	80.0	0.25	1.08	0.75	17	1.10	−9.4	139	no
P-2	86.7	0.42	1.10	0.99	23	1.05	−66.5	171	no
P-3	94.7	0.73	1.11	1.72	40	1.04	−125.2	191	no
P-4	79.5	0.86	1.17	2.29	53	1.04	−157.6	192	yes
P-5	81.4	0.93	1.20	2.57	60	1.05	−161.7	193	yes
P-6	69.6	1.07	1.15	3.00	70	1.10	−157.7	194	yes
P-7	73.9	1.50	1.17	3.41	80	1.07	−162.5	194	yes
P-8	84.3	2.18	1.33	5.42	126	1.03	−154.0	195	yes
P-9[b]		9.44	1.52	13.89	326	1.29	−168.9	198	yes

[a] Polymerization condition: anisole solution (50 wt %); temperature, 90 ± 0.5 °C; initiating system, ethyl 2-bromo-2-methylpropanoate/CuBr/*N*,*N*,*N*′,*N*′,*N*″-pentamethyldiethylenetriamine (1:1:1, molar ratio). [b] Polymerization condition: anisole solution (30 wt %); temperature, 90 ± 0.5 °C; initiator, benzoyl peroxide (0.25%, based on total mole numbers of monomers). [c] Number-average molecular weight ($M_{n,GPC}$), weight-average molecular weight ($M_{w,GPC}$), and polydispersity distribution index ($PDI_{GPC} = M_{w,GPC}/M_{n,GPC}$) were obtained by gel permeation chromatography, calibrated against a series of monodispersed polystyrene standards. [d] Absolute number-average molecular weight ($M_{n,GPC-LS}$), weight-average molecular weight ($M_{w,GPC-LS}$), and polydispersity distribution index ($PDI_{GPC-LS} = M_{w,GPC-LS}/M_{n,GPC-LS}$) were estimated at 35 °C using a GPC−light scattering online technique. [e] Degree of polymerizations were calculated from $M_{n,GPC-LS}$. [f] Specitic optical rotations were measured in THF at 20 °C THF. Concentration: $c = 2.0$ g L^{-1}. Solvent: THF. [g] Glass transition temperatures were obtained from the second heating differential scanning calorimetry thermograms.

h by breaking the tube. The reaction mixture was diluted with 20 mL of THF and was allowed to pass through a short Al_2O_3 column. The crude product was obtained by adding the filtrate into 300 mL of methanol under rapid stirring and collection of precipitate by filtration. The operations of dissolution in THF and precipitation in methanol were repeated three times to remove unreacted monomer. After being dried at 50 °C under vacuum, 0.87 g of PMBPS was obtained. The monomer conversion in weight was 87%.

Radical Copolymerization. Copolymerization of MBPS with St was carried out in anisole at 80 °C. In a typical run, MBPS (0.62 g, 1.44 mmol), St (0.15 g, 1.5 mmol), BPO (3.80 mg, 0.01 mmol), and anisole (1.23 g, 11.38 mmol) were introduced into a reaction glass tube. After three freeze−pump−thaw cycles, the tube was sealed under vacuum and put into a thermostated oil bath at 80 °C. The reaction was allowed to continue for 30 min and terminated by breaking the tube. The reaction mixture was diluted with 10 mL of THF and then precipitated into 200 mL of methanol. The operations of dissolution in THF and precipitation in methanol were repeated three times to remove unreacted monomers. After being dried at 50 °C under vacuum, 0.10 g of copolymer was obtained. The conversion in weight was 13.8%. ^{1}H NMR (δ, ppm, methylene chloride-d_2): 0.6−3.0 (broad peaks, $-CH_2CH-$ protons of the backbone and $-CH(CH_3)CH_2CH_3$ protons in the side groups of MBPS), 3.2−4.5 (broad peaks, $-OCH_2-$ protons in the side groups of MBPS), 5.6−8.0 (broad peaks, aromatic protons of MBPS and St).

Instruments and Measurements. Optical rotations were measured on a Jasco P-1030 polarimeter in a 5 cm cell at 20 °C with THF as solvent. CD spectra were recorded on a Jasco J-810 spectropolarimeter in a 1 cm cell using THF as solvent at 20 °C and analyzed by the associated J800 software. The sample concentration was 10^{-5} mol/L. ^{1}H NMR spectra were obtained with a Bruker ARX 400 MHz NMR spectrometer with CD_2Cl_2 as the solvent and tetramethylsilane as the internal reference.

The number-average molecular weight ($M_{n,GPC}$), weight-average molecular weight ($M_{w,GPC}$), and polydispersity distribution index (PDI_{GPC}, $M_{w,GPC}/M_{n,GPC}$) of the resultant homopolymers and copolymers were estimated on a gel permeation chromatography (GPC) instrument equipped with a Waters 515 HPLC pump and a Waters 2410 refractive-index detector. Three Waters Styragel columns with 10 μm bead size were connected in series. Their effective molecular weight ranges were 100−10 000 for Styragel HT2, 500−30 000 for Styragel HT3, and 5000−600 000 for Styragel HT4, respectively. The pore sizes are 50, 100, and 1000 nm for Styragels HT2, HT3, and HT4, respectively. THF was used as the eluent at a flow rate of 1.0 mL/min at 35 °C. The calibrating curve was made with the polystyrene standards.

The absolute number-average molecular weight ($M_{n,GPC-LS}$), weight-average molecular weight ($M_{w,GPC-LS}$), and polydispersity distribution index (PDI_{GPC-LS}, $M_{w,GPC-LS}/M_{n,GPC-LS}$) of the homopolymers were characterized by the same GPC instrument mentioned above except that the Waters 2410 refractive-index detector was replaced by a Wyatt Technology DAWN HELEOS 18 angle (from 15 to 165 °) light scattering detector using a Ga−As laser (658 nm, 40 mW). The concentration at each elution volume was determined with a Wyatt Optilab Rex interferometeric differential refractometer (658 nm). The molecular weight data were calculated using Astra 5.1.6.0 software (Wyatt Technology). The refractive index increment (dn/dc) of PMBPS was estimated as 0.186 mL/g in THF at room temperature by an Optilab Rex interferometeric refractometer (Wyatt Technology) at the wavelength of 658 nm. The sample concentrations were 2.0, 4.0, 6.0, 8.0, 10.0, 12.0, and 14.0 mg/mL, respectively. The refractometer was calibrated with aqueous NaCl solutions. All samples were dissolved in THF and stayed overnight before filtration for use through a 0.45 μm PTFE filter.

Differential scanning calorimetry (DSC) spectra were recorded on a TA DSC Q100 calorimeter in a temperature range of 0 to 280 °C at a heating 20 °C /min under continuous nitrogen flow. To observe the glass transition clearly, all the samples were cooled at a cooling rate of 2 °C/min from 280 to 0 °C first. Thermogravimetric analyses (TGA) were performed on a TA SDT 2960 instrument with a heating rate of 10 °C /min until 600 °C. Mesophase textures were examined on a Leica DML polarized light optical microscope with a Linkam TH-600PM hot stage. The sample films were prepared by the solution-cast method, and the thickness was kept at several micrometers.

One-dimensional wide-angle X-ray diffraction (1D-WAXD) powder experiments were performed on a Philips X'Pert Pro diffractometer with a 3 kW ceramic tube as the X-ray source (Cu Kα) and an X'celerator detector. The sample stage was set horizontally. The reflection peak positions were calibrated with silicon powder ($2\theta > 15°$) and silver behenate ($2\theta < 10°$). Background scattering was recorded and subtracted from the sample patterns. A temperature control unit (Paar Physica TCU 100) in conjunction with the diffractometer was utilized to study the structure evolutions as a function of temperature. The heating and cooling rates in the WAXD experiments were 10 °C/min.

Two-dimensional wide-angle X-ray diffraction (2D-WAXD) fiber patterns were obtained using a Bruker D8 Discover diffractometer with general area detector diffraction system (GADDS) as a 2D detector. Again, calibrations were conducted against silicon powder and silver behenate. Samples were mounted on the sample stage, and the point-focused X-ray beam was aligned either perpendicular or parallel to the mechanical shearing direction. Fibers were drawn with stretching at a rate of about 1 m s^{-1} at 280 °C and quenched to room temperature for measurements. The 2D WAXD patterns were recorded in a transmission mode at room temperature.

Table 2. Copolymerization Results of (+)-2,5-Bis[4-((*S*)-2-methylbutoxy)phenyl]styrene with Styrene and Properties of the Resultant Copolymers

copolymers[a]	m_{MBPS}[b]	convn (%)	$M_n \times 10^{-4}$ [c]	PDI[c]	$[\alpha]_{365}^{20}$ [d] (deg)	T_g[e] (°C)	liquid crystallinity
MBPS(0.05)-*co*-St(0.95)		8.2	2.86	1.61	8.5	107	no
MBPS(0.10)-*co*-St(0.90)	0.10	7.5	2.99	1.58	13.5	110	no
MBPS(0.20)-*co*-St(0.80)	0.19	3.4	3.43	1.62	21.5	121	no
MBPS(0.29)-*co*-St(0.71)	0.27	11.9	4.65	1.55	30.8	132	no
MBPS(0.39)-*co*-St(0.61)	0.34	12.1	4.83	1.64	39.6	143	no
MBPS(0.49)-*co*-St(0.51)	0.44	13.8	6.27	1.53	41.4	157	no
MBPS(0.59)-*co*-St(0.41)	0.54	6.1	6.04	1.55	48.1	168	no
MBPS(0.69)-*co*-St(0.31)	0.65	14.2	8.67	1.43	46.4	181	no
MBPS(0.79)-*co*-St(0.21)	0.76	12.3	9.51	1.43	39.8	192	no
MBPS(0.90)-*co*-St(0.10)		14.2	4.50	1.56	9.4	198	no
MBPS(0.95)-*co*-St(0.05)		2.7	2.66	1.57	−30.0	201	no
MBPS(0.98)-*co*-St(0.02)		2.7	1.48	1.70	−51.6	193	no
MBPS(0.99)-*co*-St(0.01)		12.2	2.50	1.67	−106.4	194	yes
PS	0	2.5	2.77	1.60		107	no
PMBPS	1	/	9.44	1.52	−168.9	198	yes

[a] Polymerization condition: anisole solution (50 wt %); temperature, 80 ± 0.5 °C; initiator, benzoyl peroxide (0.5%, based on total mole numbers of monomers). The numbers in the parentheses indicate the molar fraction of each monomer in feed. [b] m_{MBPS}: Molar fractions of MBPS in the copolymers obtained from ^{1}H NMR spectroscopy. [c] Number-average molecular weight (M_n), Weight-average molecular weight (M_w) and polydispersity distribution index (M_w/M_n) were obtained from gel permeation chromatography, calibrated against a series of monodispersed polystyrenes standards. [d] Specitic optical rotations were measured on a Jasco P-1030 polarimeter in THF at 20 °C. Concentration: $c = 2.0$ g L^{-1}. Solvent: THF. [e] Glass transition temperatures were obtained from the second heating differential scanning calorimetry curves.

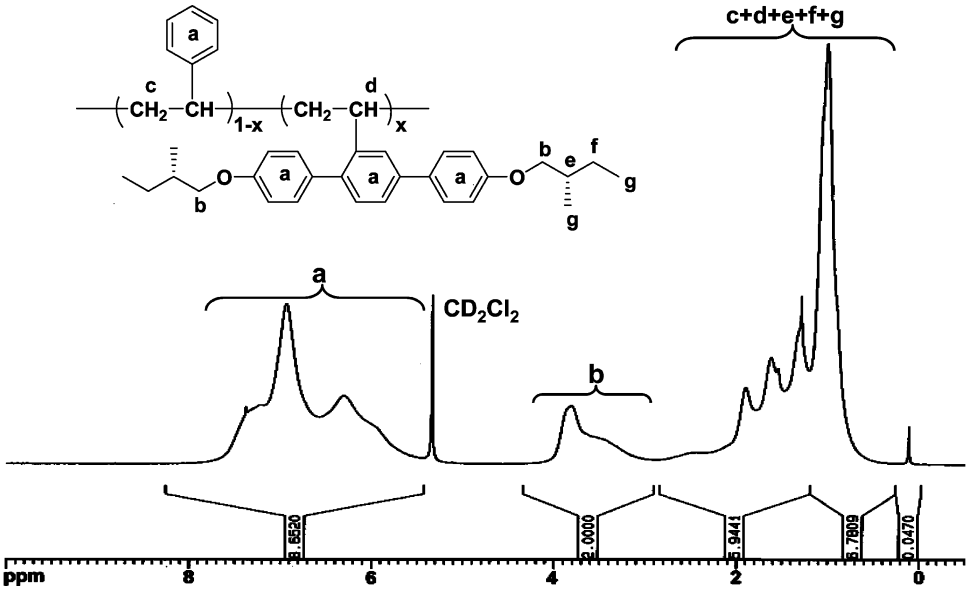

Figure 1. ^{1}H NMR spectrum of a representative copolymer MBPS(0.49)-*co*-St(0.51) (methylene chloride-d_2, 400 MHz).

Results and Discussion

Polymerization. MBPS homopolymers were prepared via ATRP in anisole at 90 °C using EBMP/CuBr/PMDETA (1:1:1, molar ratio) as the initiating system. The polymerization time was 24 h. The MWs were adjusted by changing the ratio of monomer to initiator. The resultant polymers were characterized by both GPC and GPC-LS. The results are depicted in Table 1. It is evident that DPs determined by GPC-LS were larger than those deduced from GPC. The deviation was probably caused by the fact that the hydrodynamic volumes of MBPS polymers differed substantially from those of the polystyrene standards. The quite wide $M_{n,GPC-LS}$ range from 0.75×10^4 to 1.39×10^5 allowed systematic investigations on the dependences of chiroptical and thermotropic properties on the MWs.

Copolymerization. Copolymers of MBPS with St were obtained through conventional radical polymerization employing BPO as the initiator. The copolymers were abbreviated as MBPS(x)-*co*-St($1 - x$), where x and $1 - x$ in the parentheses denoted the molar fraction of each monomer in the feed. To minimize the effect of unequal monomer consumption during the process of copolymerization, the monomer conversions were kept below 15%. The copolymerization results are summarized in Table 2. The feed molar content of MBPS ranged from 0.05 to 0.99. The chemical compositions of the copolymers were estimated by ^{1}H NMR spectroscopy with CD_2Cl_2 as the solvent. Figure 1 shows the ^{1}H NMR spectrum of a representative copolymer MBPS(0.49)-*co*-St(0.51). The assignments of resonance peaks could be seen from the figure. The molar contents of MBPS (m_{MBPS}) and St (m_{St}) in copolymers were calculated according to

$$4m_{MBPS}/(11m_{MBPS} + 5m_{St}) = I_{oxymethylene}/I_{aromatic} \quad (1)$$

$$m_{MBPS} + m_{St} = 1 \quad (2)$$

where $I_{oxymethylene}$ and $I_{aromatic}$ were defined as the relative intensities of resonance peaks of $-OCH_2-$ protons in MBPS unit and aromatic protons in both MBPS and St units, respectively.

It should be pointed out that because the resolution of 400 MHz NMR instrument we used was not high enough, the peaks of $-OCH_2-$ overlapped slightly with other aliphatic protons and those of the residual CH_2Cl_2 in CD_2Cl_2 solvent with

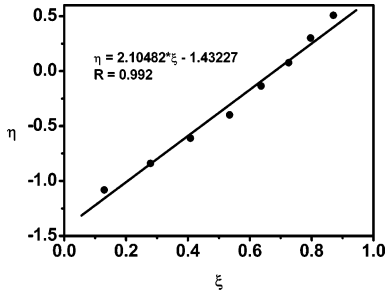

Figure 2. Kelen−Tudos (K−T) linearization method plots based on ^{1}H NMR results.[51]

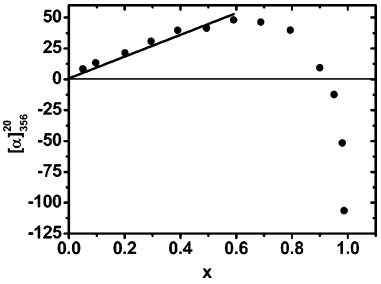

Figure 3. Specific optical rotations of the copolymers vs the feed molar content of MBPS (*x*).

aromatic protons, which limited the accuracy of measurement, m_{MBPS} and m_{St} estimated by ^{1}H NMR spectra became less reliable when the molar fraction of MBPS or St was too high. Therefore, only were the compositions of eight copolymers with *x* values ranging from 0.10 to 0.79 presented. In addition, the copolymerization was carried out at 80 °C instead of at 90 °C as in ATRP since BPO decomposed too fast at 90 °C, if no mediation was applied, to allow easy control of the monomer conversion under 15%, although the resultant PMBPS usually exhibits the larger optical rotation for compound obtained at a higher temperature than at a lower temperature.[55]

Reactivity Ratio. The Kelen−Tudos (K−T) linearization method was chosen to estimate the monomer reactivity ratios of MBPS (r_{MBPS}) and St (r_{St}) based on the monomer feed ratios and the copolymer compositions.[56] In the K−T method, M_1 and M_2 represent the concentrations of the two comonomers. At low conversion, dM_1 and dM_2 correspond to the concentration ratio of the copolymer components. *x* and *y* are defined as M_1/M_2 and dM_1/dM_2, respectively. The transformed variables are defined as

$$\eta = \frac{G}{\alpha + F} \quad \text{and} \quad \xi = \frac{F}{\alpha + F} \tag{3}$$

where *G* and *F* are defined as $x(y-1)/y$ and x^2/y, separately. And α is $\sqrt{F_m F_M}$, where F_m and F_M stand for the lowest and the highest values of *F*, respectively. The linearization version of copolymer equation is defined in the K−T linearization method:

$$\eta = r_1\xi - \frac{r_2}{\alpha}(1-\xi) \tag{4}$$

Figure 2 shows the corresponding K−T method plots. By extrapolating ξ to 0 and 1, r_{MBPS} and r_{St}were determined as 0.67 and 0.98, respectively. The value of $r_{MBPS} \times r_{St}$ was close to 1, indicating the two monomer units had a tendency of random distribution in the polymer chain and no significant heterogeneity existed.[49,57]

The fact of $r_{MBPS} < r_{St}$ implied that St was more reactive than MBPS in radical copolymerization. This was quite different from the copolymerizations of St with other bulky styrenic monomers similar to MBPS. For example, when MPCS copolymerized with St, MPCS showed much higher reactivity ($r_{MPCS} = 4.15$) than St ($r_{St} = 0.44$), which was attributed to the electron-withdrawing effect of ester groups and conjugate effect.[49] Ober and co-workers noticed the similar behavior in nitroxide-mediated free radical polymerization of 2,5-bis[(4-butylbenzoyl)oxy]styrene (BBOS).[58] In bulk, BBOS polymerized much faster than its nonmesogenic, electron deficient model, 2,5-diacetoxystyrene; whereas in a dilute solution, the polymerization rates of both monomers were comparable. The increased reactivity of BBOS in bulk was attributed to the presence of a nematic phase, which led to localized ordering of the monomers. For the system of MBPS and St, we considered the relatively lower reactivity of the former than the later might be rationalized by the steric hindrance of bulky terphenyl side groups and the electron-donor effect of alkoxy groups, the later of which made the MBPS-ended radical less stable.

Chiroptical Properties. It has been known that the backbone conformation of the polymers is one of the primary factors defining their phase behavior and associated material properties. The MW dependence of conformation relies significantly on the main-chain rigidity.[41] The flexible polymers with low MWs take extended global shape, while those with high-MWs adopt a random-coil conformation in solution and in an isotropic melt or solid. The MWs have less influence on the conformation in rigid main-chain polymers than in flexible polymers. The typical examples are rodlike MC-LCPs.[1] However, for some polymers with a flexible backbone, their conformations changed from random-coiled and spherical to extended and cylindrical with increasing MWs when being densely grafted by self-assemblying flat-tapered monodendrons, polymer chains and bulky side groups.[39−43,59,60]

The specific optical rotations $[\alpha]_{365}^{20}$ of PMBPS relied remarkably on MW (Table 1).[61] The monomer MBPS had a positive $[\alpha]_{365}^{20}$ of +60.4°, while the corresponding polymer with DP exceeding 53 had $[\alpha]_{365}^{20}$ of about −160°. The opposite sign of optical rotation of polymer to monomer and the large increase in magnitude could be understood as arising from a chiral higher structure, most likely stable helical conformation of the vinyl backbone with a predominance of one screw sense. In the DP range from 17 to 53, the optical rotation of the polymer grew with an increase in MW, reflecting the gradual development and stabilization of rigid helical chain structure.[60,62−64]

Figure 3 shows the $[\alpha]_{365}^{20}$ dependence of MBPS(*x*)-*co*-St(1 − *x*) on the composition. When $x < 59\%$, the $[\alpha]_{365}^{20}$ values of the copolymers increased linearly with the feed molar content of MBPS as in the mixture of MBPS and St, indicating no new chiral structure formed in the copolymers and their optical activities originated solely from the chiral centers of side groups in MBPS units.[65] Increasing the MBPS content further, $[\alpha]_{365}^{20}$ values declined but were still positive, an indicative of the formation of a new chiral secondary structure with opposite optical rotation as PMBPS. When *x* reached above 90%, the optical rotations of copolymers became negative and increased sharply with increasing *x*. It suggested that the contribution to optical rotation from the newly formed chiral structure was dominant in the copolymers with high MBPS content.

The CD spectra of copolymers in THF at 20 °C are shown in Figure 4. When *x* was less than 59%, the Cotton effects of the copolymer were very similar to those of MBPS and its model compound, exhibiting just weak positive Cotton effects at around 272 nm. In the case of the copolymers with *x* exceeding 59%,

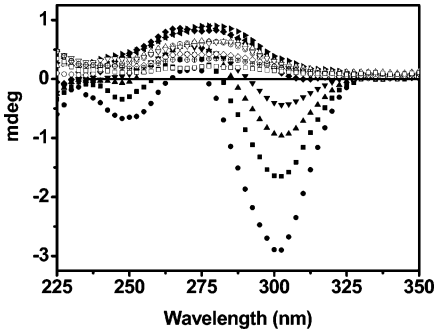

Figure 4. Circular dichroism spectra of the copolymers with various compositions (recorded at 20 °C in THF, $c = 0.025$ g/L). The molar contents of MBPS in feed (x): 0.99 (●); 0.98 (■); 0.95 (▲); 0.90 (▼); 0.79 (◆); 0.69 (solid triangle pointing left); 0.59 (solid triangle pointing right); 0.49 (○); 0.39 (△); 0.29 (▽); 0.20 (◇); 0.10 (⊗); 0.05 (□).

the Cotton effects at 272 nm became less intensive and a new Cotton effect in the range of $\pi-\pi^*$ absorption of side terphenyl groups was observed when x reached 90%, indicating again the formation of helical chain structure with the predominance of one screw sense.[51]

Molecular Weight Dependence of Thermotropic Behavior of MBPS Homopolymers. The dependence of the thermal transition temperatures on the MWs of MBPS homopolymers was studied by DSC. The DSC thermograms of all the homopolymers were featureless except for glass transitions (not shown). In order to identify glass transition clearly, the samples were heated to 280 °C and maintained at the temperature for 5 min, followed by cooling at a rate of 2 °C/min to 0 °C and heating again at a rate of 40 °C/min, since fast heating slowly cooled samples induced endothermic hysteresis peak in glass transition region. The glass transition temperatures (T_gs) are summarized in Table 1. It was evident that T_gs increased with increasing MWs when MWs were less than 1.72×10^4 g/mol and kept almost unchanged when MWs were higher than 1.72×10^4 g/mol.

MBPS homopolymers were white powders at room temperature. Under cross-polarized light microscope, only very weak birefringence was observed presumably due to the certain ordered arrangements of polymers formed during precipitation from solution. Heating above T_gs, the polymers behaved differently depending on MWs. For the polymers with DPs smaller than or equal to 40 (i.e., P-1, P-2, and P-3), the weak birefringence seen at room-temperature disappeared upon being heated to T_gs and no birefringence developed again until thermal decomposition started, indicating no ordered structure formation in these samples. For the polymers with DPs higher than 40, the weak birefringence of as-obtained polymer powders also disappeared at glass transitions but developed again immediately. The birefringence of P-4 (DP = 53) developed was quite weak and no clear liquid crystalline texture could be observed irrespective of any thermal history and treatment (including cooling, heating, and isothermal condition), indicating a poor ordered arrangement of macromolecules. The polymers P-5 and P-6 presented typical nematic schlieren textures, suggesting the formation of nematic phase; while P-7, P-8, and P-9 yielded star-shaped textures, implying the generation of hexatic columnar nematic phase.[30] Figure 5 shows the schlieren textures of P-5 and star-shaped textures of P-7, respectively. To get a clear enough picture, the polymers were dissolved in toluene and cast onto a piece of clean cover glass. After drying thoroughly under vacuum at room temperature, the resultant films were annealed at 220 °C for at least 3 h.

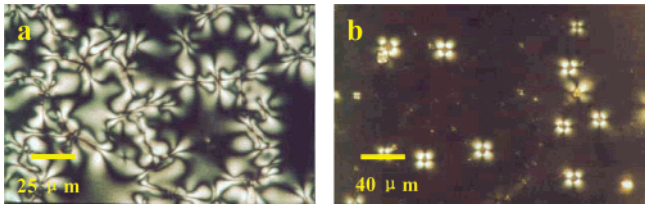

Figure 5. Polarized light optical microphotographs of PMBPS taken at 220 °C: (a) P-5, DP = 60; (b) P-9, DP = 326. The polymer films with thickness of about 10 μm were prepared by solution-cast method and annealed at 220 °C for at least 3 h before taking the pictures.

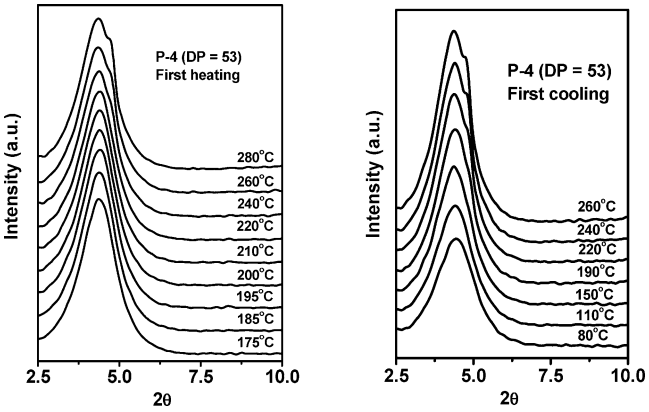

Figure 6. Temperature variable one-dimensional wide-angle X-ray diffraction powder patterns in the low 2θ angle region of PMBPS (P-4, DP = 53) recorded during the first heating and the subsequent cooling processes.

On the basis of the POM observations, MBPS homopolymers could be divided into three groups: the first group with low MWs, P-1−P-3, did not possess thermotropic LC property; the second group with intermediate MWs, P-4−P-6, formed nematic mesophases; and the last group with high MWs, P-7−P-9, developed hexatic columnar nematic phase. In addition, P-4 was the sample with the critical MW to form mesophase. However, using DSC and POM only could not exactly identify the phase structure, and therefore, 1D- and 2D-WAXDs were carried out to investigate the phase structures of the representative samples.

The temperature variable 1D-WAXD powder patterns of the three polymers with low MWs, P-1−P-3, were the same. There were two scattering halos in low- and wide-angle regions, which intensified slightly by raising temperature but remained broad in the whole temperature range studied, i.e., 30−280 °C, suggesting that no ordered structure developed.

Figure 6 depicts the temperature variable 1D-WAXD powder patterns of the polymer P-4 at a low 2θ angle. It was known in the previous section that the sample could only develop faint birefringence above T_g. In 1D-WAXD curves, P-4 presented only broad scattering below 260 °C. Above the temperature, a shoulder peak in the right side of the original scattering halo ($2\theta = 4.75°$) grew up and remained until thermal decomposition. The shoulder disappeared when the sample was cooled below 240 °C during the subsequent cooling process. The results implied that the order of the suprastructure formed by P-4 was poor due to low MW and the mesophase formation was reversible. This was in consistent with the POM observation.

Temperature variable 1D-WAXD patterns of as-cast P-5 and P-9 samples in the low 2θ (between 2.5 and 10°) angle regions recorded during the first heating and the subsequent cooling runs are shown in Figure 7 and 8, respectively. A scattering halo was observed below 230 °C, which meant only short-range order existed on the supramolecular length scale and the sample was in amorphous state. Above 230 °C, sharp reflection peaks

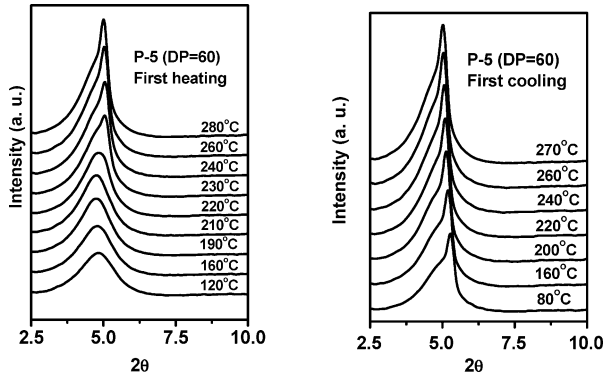

Figure 7. Temperature variable one-dimensional wide-angle X-ray diffraction powder patterns in the low 2θ angle region of PMBPS (P-5, DP = 60) recorded during the first heating and the subsequent cooling processes.

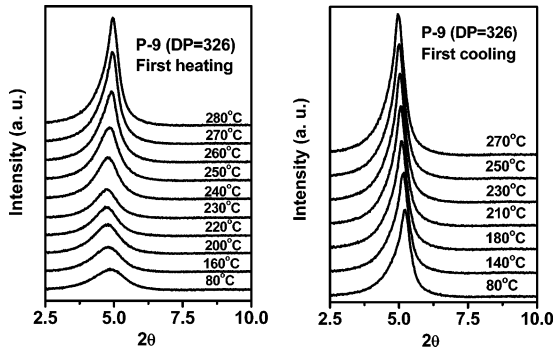

Figure 8. Temperature variable one-dimensional wide-angle X-ray diffraction powder patterns in the low 2θ angle region of PMBPS (P-9, DP = 326) recorded during the first heating and the subsequent cooling processes.

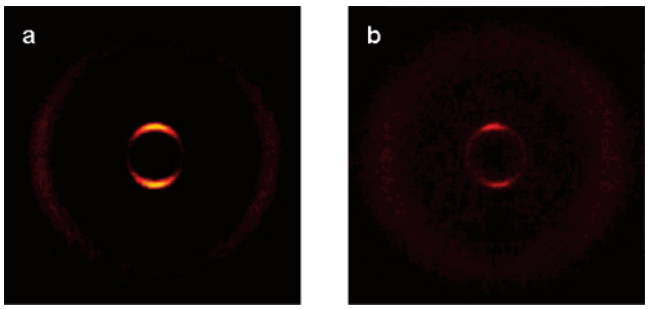

Figure 9. Two-dimensional wide-angle X-ray diffraction fiber patterns of PMBPS: (a) P-5, DP = 60; (b) P-9, DP = 326. The X-ray incident beam was perpendicular to the oriented film.

center at $2\theta = 4.75$ and 5.03° (d spacings of 1.86 and 1.75 nm) for P-5 and P-9, respectively, developed from the scattering halos, implying that the order structures on the supramolecular length scale formed.[35,37] The reflection peaks became intensive and shifted slightly and continuously with increasing temperature toward low 2θ angle due to thermal expanding. When cooled slowly from 280 °C, the sharp reflection peaks became less intensive in the intensities with reducing temperature but did not disappear until room temperature. The polymer P-6 had similar 1D-WAXD power patterns to P-5, while the polymers P-7 and P-8 had similar 1D-WAXD power patterns to P-9. No high order diffraction was observed.

We used 2D-WAXD to further investigate the phase structures of the polymers P-5−P-9. Figure 9a shows the 2D-WAXD pattern of the oriented P-5 sample with the X-ray incident beam perpendicular to the orientation direction (equator direction). A pair of strong diffraction arcs were present on the meridian at $2\theta = 5.04°$ (d spacing of 1.75 nm), implying the ordered structure developed along the direction perpendicular to the fiber axis on the nanometer scale.[35] In the high 2θ angle region, a scattering halo appeared on the equator at $2\theta = 19.32°$ (d spacing of 0.46 nm) with a broad azimuthal distribution, which indicated only that the short-range order existed along the orientation direction. Except for a pair of strong diffraction arcs displayed in the low 2θ angle region, there was no higher order diffraction identified even after a prolonged exposure time. Figure 9b exhibits the 2D WAXD pattern of the oriented P-9 sample with the X-ray beam perpendicular to the fiber axis. It was similar to that of P-5. The d-spacing corresponding to the meridian diffraction arcs was 1.67 nm ($2\theta = 5.24°$), a little smaller than P-5, suggesting the macromolecules of P-9 packed closer than those of P-5 and had a higher supramolecular order.

Parts a and b of Figure 10 show the diffraction patterns of the oriented P-5 and P-9, respectively, with the shearing direction parallel to the X-ray incident beam. P-5 presented a ring pattern centered at $2\theta = 5.04°$ (d spacing of 1.75 nm). Azimuthal scanning gave an isotropic intensity distribution (Figure 10c). Therefore, the liquid crystalline structure of P-5 should be Φ_N phase.[35] In the case of P-9, 6-fold symmetric diffraction arcs were displayed at $2\theta = 5.24°$ (d spacing of 1.67 nm) (Figure 10b). There were six almost identical maxima intensity with 60° angle between the two adjacent diffraction maxima in the azimuthal scanning curves. It meant that P-9 in the LC state was a hexagonal lateral packing of the cylinders, and the average diameter of each cylinder was 1.67 nm. Because it was lacking higher order diffractions, the hexagonal lateral packing did not possess the long-range order perpendicular to the oriented sample. Therefore, the liquid crystalline phase of P-9 should be assigned as hexatic columnar nematic (Φ_{HN}) phase.[35] The phase structure of P-6 was the same with P-5, while those of P-7 and P-8 were the same with P-9.

Composition Dependence of Thermotropic Behaviors of Copolymers. Figure 11 exhibits the second heating DSC traces of the copolymers. All the samples displayed single glass transition, indicating the random distribution of the two monomer units along the copolymer main chain and no discernible phase separation occurred. This was consistent with the results made based on monomer reactivity radios. The T_gs of the copolymers increased at first and then decreased with increasing MBPS content. A similar phenomenon was observed in the copolymer system based on MPCS and St.[49] It might be due to the fact that the favorable interaction between the two structural units in the copolymers got to a maximum value at certain composition which caused a reduction in the free volume. However, there is a lot to do before a valid explanation can be made.

Similar to PMBPS, all the copolymers were white solids at room temperature and became soft above T_gs. Pressing the sample slightly, birefringence developed due to orientation but disappeared after the force was withdrawn for most of the samples with the exception of MBPS(0.99)-*co*-St(0.01), indicating that the incorporation of a very small amount of St would destroy the ordered arrangement of the copolymer molecules. These phenomena showed that most of the copolymers did not possess thermotropic LC property. The as-cast film of the copolymer MBPS(0.99)-*co*-St(0.01) was transparent and showed no birefringence under cross-polarized light microscope. When the temperature was raised above T_g, birefringence developed. Figure 12 exhibits the nematic schlieren texture of MBPS(0.99)-*co*-St(0.01) taken at 220 °C. The texture remained unchanged until thermal decomposition. Cooling the sample slowly before

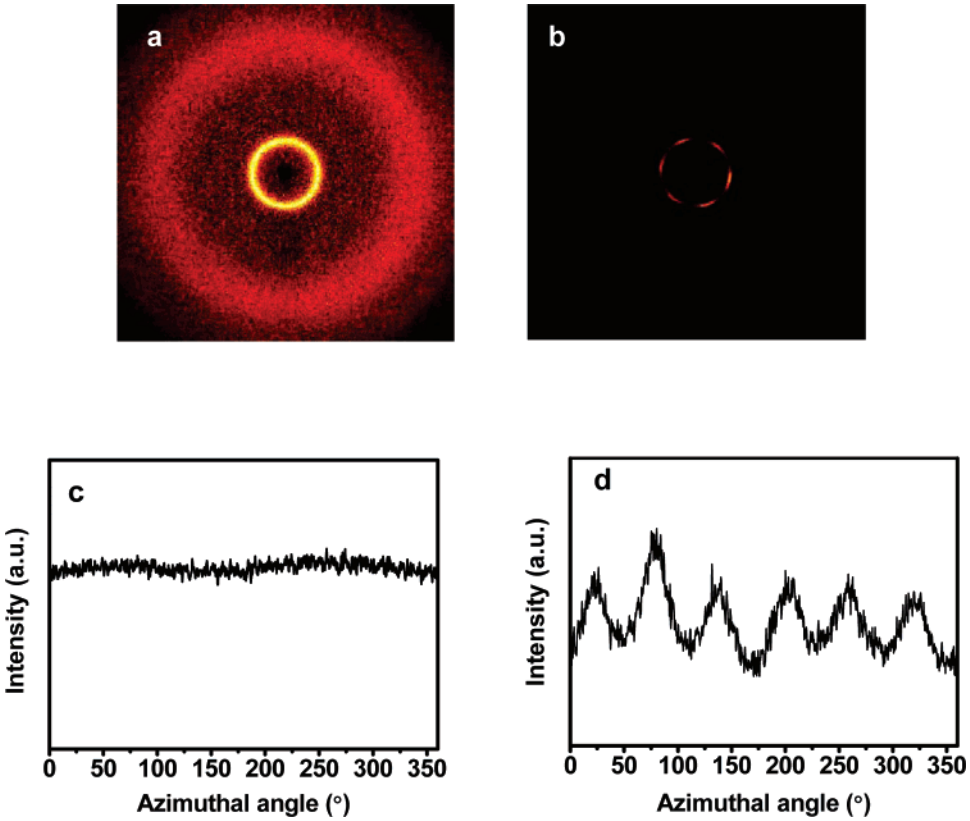

Figure 10. 2D wide-angle X-ray diffraction fiber patterns of PMBPS: (a) P-5, DP = 60; (b) P-9, DP = 326; (c and d) azimuthal scanning data of the low 2θ angle region diffractions of parts a and b, respectively. The X-ray incident beam was along the shearing direction.

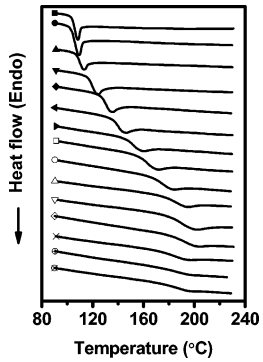

Figure 11. Differential scanning calorimetry curves of the copolymers with various compositions and homopolymers MBPS and St during the second heating scanning at a heating rate of 40 °C/min. The molar contents of MBPS in feed: 0.00 (■); 0.05 (●); 0.10 (▲); 0.20 (▼); 0.29 (◆); 0.39 (solid triangle pointing left); 0.49 (solid triangle pointing right); 0.59 (□); 0.69 (○); 0.79 (Δ); 0.90 (▽); 0.95 (◇); 0.098 (×); 0.99 (⊕); 1.00 (⊗).

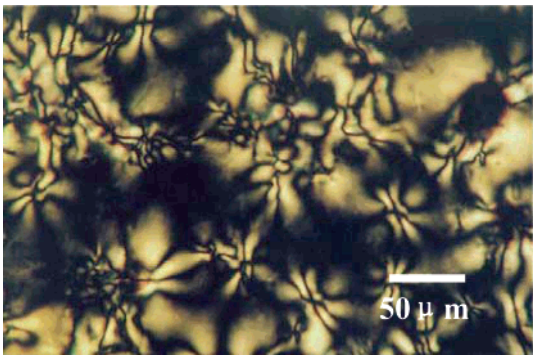

Figure 12. Polarized light optical microphotograph of MBPS(0.99)-*co*-St(0.01) taken at 220 °C. The copolymer film with thickness of about 10 μm was prepared by solution-cast method and annealed at 220 °C for at least 3 h before taking the pictures.

thermal decomposition happened resulted in no discernible texture change, indicating that the nematic phase was stable, once formed.

The temperature variable 1D-WAXD powder patterns of as-cast MBPS(0.99)-*co*-St(0.01) sample in the low 2θ (between 2.5 and 10°) angle region recorded during the first heating and the subsequent cooling runs are shown in parts of a and b of Figure 13, respectively. During heating process only an amorphous scattering halo centered at $2\theta = 4.70°$ was observed below 220 °C. At 240 °C, a new reflection peak centered at $2\theta = 4.98°$ (d spacing of 1.77 nm) developed from the scattering halo, which meant that the ordered structure on the scale of supramolecular length scale formed. The reflection peak became sharp and intense with raising temperature. When cooled slowly from 280 °C, the intensity of the reflection peak decreased and the peak shifted continuously and slightly to a high 2θ angle due to thermal shrinking.

The 2D-WAXD patterns of the oriented MBPS(0.99)-*co*-St-(0.01) sample were similar to those of the homopolymer P-5 (Figure 14). When the X-ray incident beam was perpendicular to the shearing direction (equator direction), a pair of strong diffraction arcs appeared at $2\theta = 5.08°$ (d spacing of 1.74 nm) on the meridian and a pair of scattering halos on the equator (Figure 14a), suggesting the formation of nanoscale ordered structure along the direction perpendicular to the fiber axis and only short-range order existing along the fiber direction. Figure 14b shows the 2D-WAXD pattern with the X-ray incident beam parallel to the orientation, which was used to determine the symmetry of the formation suprastructure. A ring pattern at $2\theta = 5.08°$ (d spacing of 1.74 nm) was seen. Azimuthal scanning data exhibited an isotropic intensity distribution (Figure 14c).

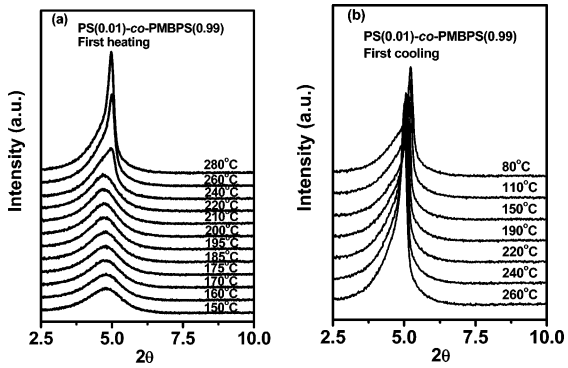

Figure 13. Temperature variable one-dimensional wide-angle X-ray diffraction patterns in the low 2θ angle region of the copolymer MBPS-(0.99)-*co*-St(0.01) recorded during the first heating and the subsequent cooling processes.

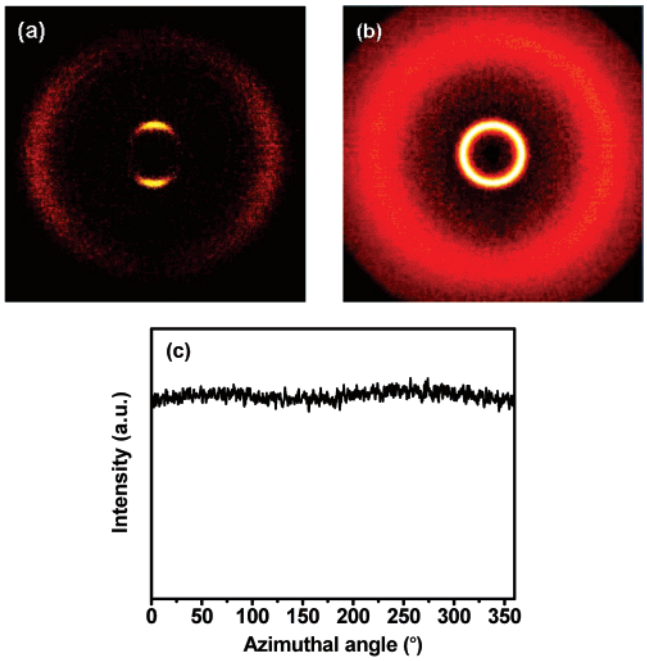

Figure 14. Two-dimensional wide-angle X-ray diffraction fiber patterns of the copolymer MBPS(0.99)-*co*-St(0.01). The X-ray incident beam was (a) perpendicular to the oriented film and (b) along the shearing direction. (c) Azimuthal scanning data of the low 2θ angle region diffractions.

The LC phase of MBPS(0.99)-*co*-St(0.01) was thus identified as a columnar nematic (Φ_N) structure.[35]

Mechanism of Mesophase Formation of PMBPS. We tried to understand the mesophase origin of PMBPS by correlating the development of helical conformation and the generation of ordered supramolecular structure. From the chiroptical property studies, it was evident that the chiral secondary structure with negative optical rotation had developed in MBPS oligomer with DP of as low as 17. The growth in $[\alpha]_{365}^{20}$ of PMBPS with MW in the low DP range and reaching a plateau at DP = 53 reflected that the stable helical conformation started at this point. The value was the same with the critical DP for PMBPS to generate a Φ_N phase. As a result, it was reasonable to consider the building blocks of mesophase of PMBPS were cylindrical columns made up of individual macromolecule taking helical conformation. In addition, in order to stabilize the mesophase, the size of the helical chain should be large enough. This could be rationalized by Flory's lattice model as described below.[66]

According to Flory's lattice theory, the critical aspect (length to diameter) ratio for a rodlike macromolecule to achieve a mesophase is 5.44, if taking into account of geometry factors exclusively. On the basis of this model, Chen et al. explained the MW dependence of mesomorphic property of PMPCS, a similar MJLCP to PMBPS studied in the present work.[35] They considered the scattering halos at large diffraction angle reflected the short-range ordered structure along the chain axis. By taking the assumption of the projection length of 0.20−0.23 nm on the helical axes of each repeating unit of isotactic bulky vinyl polymers proposed by Wunderlich[67] and comparing with the short-range ordered periodicity (0.415 nm) of poly[di(4-heptyl)-vinylterephthalate] in Φ_H state corresponding to the average distance between every two repeating units along the chain axis, the critical DPs for PMPCS to generate Φ_N and Φ_{HN} phases were estimated as 39 and 42, respectively. Applying the same method, we determined the critical DP of 42 for PMBPS to generate a Φ_N, which were slightly larger than those of PMPCS presumably due to the size difference of the side groups of the two polymers. The experimentally obtained value was 53. The deviation of the calculated value from the experimentally obtained one might account for the other factors besides geometric consideration played an important role in forming a mesophase.

The effect of the composition on the chiroptical and thermotropic properties of MBPS and St copolymers agreed well with the above argument on the origin of mesophase formation of PMBPS. Helical homopolymers may consist of a certain amount of right- and left-handed blocks separated by helical reversals.[68] The reversal can be the energy accumulation in the chain and/or the defect from the mistakes in the polymerization mechanism. In the case of copolymers, the presence of unlike units provides additional chain defects. For MBPS(x)-*co*-St(1 − x), when $x < 59\%$, the MBPS segment is too short to take an extended helical conformation due to the isolation of St unit or microsegment and their optical activities originate solely from the chiral centers of side groups in MBPS units; when $x > 59\%$, the MBPS segment is long enough to develop a helical structure with opposite optical rotation to the monomer. Increasing x has the effect to increase the length of MBPS segment and produce more stable helical conformation. When x reaches above 90%, the contribution to optical rotation from helical conformation over compensate that of asymmetric atoms in the side groups and the optical rotation of the copolymer therefore becomes negative. The fact that only one copolymer with $x = 99\%$ possesses thermotropic liquid crystallinity indicates that although helical segment is formed when $x > 59\%$, it is not long enough to generate and stabilize a mesophase.

In the side-chain liquid crystalline copolymers with flexible spacers, the mesophase is formed by the self-organization of individual mesogens in the side chains. The introduction of comonomer has the effect to reduce the concentration of mesogens. Unless the concentration is too dilute for mesogens to self-organize, the mesophase forms. For MJLCPs such as PMBPS, the main chains and side chains cooperate to form helical cylinders, which act as the building blocks of mesophase. The incorporation of St units into PMBPS main chains makes MBPS segment cannot take extended conformation or limit the length of extended structure. Either effect interrupts the formation of the mesophase. The mesophase sensitivity of MJLCPs to copolymerization can thus be understood.

One may ask that if PMBPS and PMCPS are similar in both macromolecular and mesomorphic structures, why are the maximum amounts of the same comonomer St they can tolerate to generate a mesophase so different (1% for the former, 14% for the latter)? We think the difference in the critical St content

for the corresponding copolymers to develop a mesophase do not differ so much as it seems like. In the copolymerization system of MCPS and St, the former monomer is more reactive than the later. The feed St molar content for the copolymer to achieve a mesophase is 14%, but the measured St content is just 6%. For the copolymers consisting of MBPS and St, the former monomer is less reactive than the later. Although we do not know the real composition of MBPS(0.99)-*co*-St(0.1) due to the difficulty in experiment, the molar St fraction in the copolymer should be more than 1%.

Conclusion

We have synthesized a series of MBPS homopolymers with varying MWs ($M_{n,GPC-LS} = 0.75-13.89 \times 10^4$) and relatively narrow MW distributions ($PDI_{GPC-LS} = 1.03-1.29$) via ATRP and MBPS(x)-*co*-St($1 - x$) random copolymers with various compositions ($x = 0.05-0.99$) via conventional radical copolymerization, separately. With increasing MWs, PMBPS tends to adopt a helical structure and results in the formation of Φ_N and Φ_{HN} phase depending on DP. The critical DP (=53) for PMBPS to take a stable helical backbone conformation is identical to that used to form a mesophase. The incorporation of MBPS with x values less than 59% into the copolymer main chain cannot induce a discernible helical segment. When $x >$ 59%, the formation of helical conformation of PMBPS segment with negative optical rotation is observed. Among all the copolymers, only one with x value of as high as 99% can achieve a mesophase (Φ_N). The dependences of thermotropic and chiroptical properties on the DPs of homopolymers and on the compositions of copolymers is consistent with the conclusion that a chiral secondary structure is necessary for PMBPS to form a liquid crystalline phase, but the length of the helical segment should be long enough.

Acknowledgment. The financial support from the National Natural Science Foundation of China (Grants 20674001 and 20134010) and the National Distinguished Young Scholar Fund (Grant 20325415) is gratefully acknowledged.

References and Notes

(1) Donald, A. M.; Windle, A. H. *Liquid Crystalline Polymers*; Cambridge University Press: Cambridge, U.K., 1992.
(2) Gray, G. M. In *Side Chain Liquid Crystal Polymers*; McArdle, C. B., Ed.; Chapman and Hall: New York, 1989.
(3) Magagnini, P. L.; Marchetti, A.; Matera, F.; Pizzirani, G.; Turchi, G. *Eur. Polym. J.* **1974**, *10*, 585−591.
(4) Hessel, F.; Finkelmann, H. *Polym. Bull. (Berlin)* **1985**, *14*, 375−378.
(5) Gray, G. W.; Hill, J. S.; Lacey, D. *Mol. Cryst. Liq. Cryst.* **1990**, *7*, 47−52.
(6) Finkelmann, H.; Happ, M.; Portugal, M.; Ringsdorf, H. *Macromol. Chem.* **1978**, *179*, 2541−2544.
(7) Kirste, R. G.; Ohm, H. G. *Makromol. Chem. Rapid Commun.* **1985**, *6*, 179−185.
(8) Renz, W.; Warner, M. *Phys. Rev. Lett.* **1986**, *56*, 1268−1271.
(9) Noirez, L.; Keller, P.; Cotton, J. P. *Liq. Cryst.* **1995**, *18*, 129−148.
(10) Noirez, L.; Pepy, G.; Keller, P.; Benguigui, L. *J. Phys. II* **1991**, *1*, 821−830.
(11) Wang, X. J.; Warner, M. *J. Phys. A: Math. Gen.* **1987**, *20*, 713−731.
(12) Zhou, Q. F.; Li, H. M.; Feng, X. D. *Macromolecules* **1987**, *20*, 233−234.
(13) Keller, P.; Hardouin, F.; Mauzac, M.; Achard, M. F. *Mol. Cryst. Liq. Cryst.* **1988**, *155*, 171−178.
(14) Hardouin, F.; Mery, S.; Achard, M. F.; Noirez, L.; Keller, P. *J. Phys. II* **1991**, *1*, 511−520.
(15) Hardouin, F.; Leroux, N.; Mery, S.; Noirez, L. *J. Phys. II* **1992**, *2*, 271−278.
(16) Lecommandoux, S.; Noirez, L.; Richard, H.; Achard, M. F.; Strazielle, C.; Hardouin, F. *J. Phys. II* **1996**, *6*, 225−234.
(17) Lam, J. W. Y.; Tang, B. Z. *J. Polym. Sci., Part A: Polym. Chem.* **2003**, *41*, 2607−2629.
(18) Lam, J. W. Y.; Tang, B. Z. *Acc. Chem. Res.* **2005**, *38*, 745−754.
(19) Lam, W. Y.; Kong, X.; Tang, B. Z. *Macromolecules* **2000**, *33*, 5027−5040.
(20) Ye, C.; Lam, W. Y.; Liu, Z.-F.; Cheng, S. Z. D.; Chen, E.-Q.; Tang, B. Z. *J. Am. Chem. Soc.* **2005**, *127*, 7668−7669.
(21) Tang, B. Z.; Kong, X.; Wan, X.; Feng, X.-D.; Kwok, H. S. *Macromolecules* **1998**, *31*, 2419−2432.
(22) Zhou, Q. F.; Li, Z. X.; Wen. Z. Q. *Macromolecules* **1989**, *22*, 491−493.
(23) Zhang, D.; Zhou, Q. F.; Ma, Y. G.; Wan, X. H.; Feng, X. D. *Polym. Adv. Technol.* **1997**, *8*, 227−233.
(24) Wan, X. H.; Zhou, Q. F.; Zhang, D.; Zhang, Y.; Feng, X. D. *Chem. J. Chin. Univ.* **1998**, *19*, 1507−1512.
(25) Zhang, D.; Liu, Y.; Wan, X.; Zhou, Q.-F. *Macromolecules* **1999**, *32*, 5183−5185.
(26) Zhang, D.; Liu, Y.; Wan, X.; Zhou, Q.-F. *Macromolecules* **1999**, *32*, 4494−4496.
(27) Yu, Z. N.; Tu, H. L.; Wan, X. H.; Chen, X. F.; Zhou, Q. F. *J. Polym. Sci., Part A* **2003**, *41*, 1454−1464.
(28) Chen, X.; Tenneti, K. K.; Li, C. Y.; Bai, Y.; Zhou, R.; Wan, X.; Fan, X.; Zhou, Q.-F. *Macromolecules* **2006**, *39*, 517−527.
(29) Zhou, Q. F.; Wan, X. H.; Zhu, X. L.; Zhang, F.; Feng, X. D. *Mol. Cryst. Liq. Cryst.* **1993**, *231*, 107−117.
(30) Kwolek, S. L.; Morgan, S. L.; Schaefgen, J. L.; Gulrich, L. W. *Macromolecules* **1977**, *10*, 1390−1396.
(31) Economy, J.; Volksen, W.; Viney, C.; Geiss, R.; Siemens, R.; Karis, T. *Macromolecules* **1988**, *21*, 2777−2781.
(32) Wan, X. H.; Zhang, F.; Wu, P.; Zhang, D.; Feng, X. D.; Zhou, Q. F. *Macromol. Symp.* **1995**, *96*, 207−218.
(33) Zhi, J. G.; Liu, A. H.; Zhu, Z. G.; Lü, X. C.; Fan, X. H.; Chen, X. F.; Wan, X. H.; Zhou, Q. F. *Acta Polym. Sin.* **2005**, *5*, 774−778.
(34) Xu, G. Z.; Wu, W.; Shen, D. Y.; Hou, J. N.; Zhang, S. F.; Xu, M.; Zhou, Q. F. *Polymer* **1993**, *34*, 1818−1822.
(35) Ye, C.; Zhang, H. L.; Huang, Y.; Chen, E. Q.; Lu, Y. L.; Shen, D. Y.; Wan, X. H.; Shen, Z. H.; Cheng, S. Z. D.; Zhou, Q. F. *Macromolecules* **2004**, *37*, 7188−7196.
(36) Yin, X. Y.; Ye, C.; Ma, X.; Chen, E. Q.; Qi, X. Y.; Duan, X. F.; Wan, X. H.; Cheng, S. Z. D.; Zhou, Q. F. *J. Am. Chem. Soc.* **2003**, *125*, 6854−6855.
(37) Tu, H. L.; Wan, X. H.; Liu, Y. X.; Chen, X. F.; Zhang, D.; Zhou, Q. F.; Shen, Z. H.; Ge, J. J.; Jin, S.; Cheng, S. Z. D. *Macromolecules* **2000**, *33*, 6315−6320.
(38) Gopalan, P.; Andruzzi, L.; Li, X. F.; Ober, C. K. *Macromol. Chem. Phys.* **2002**, *203*, 1573−1583.
(39) Kwon, Y. K.; Chvalun, S.; Schneider, A.-I.; Blackwell, J.; Percec, V.; Heck, J. A. *Macromolecules* **1994**, *27*, 6129−6132.
(40) Kwon, Y. K.; Chvalun, S.; Blackwell, J.; Percec, V.; Heck, J. A. *Macromolecules* **1995**, *28*, 1552−1558.
(41) Percec, V.; Ahn, C. H.; Ungar, G.; Yeardley, D. J. P.; Moller, M.; Sheiko, S. S. *Nature (London)* **1998**, *391*, 161−164.
(42) Prokhorova1, S. A.; Sheiko, S. S.; Möller, M.; Ahn, C.-H.; Percec, V. *Macrom. Rapid Commun.* **1998**, *19*, 359−366.
(43) Percec, V.; Ahn, C. H.; Barboiu, B. *J. Am. Chem. Soc.* **1997**, *119*, 12978−12979.
(44) Percec, V.; Pugh, C. In *Side Chain Liquid Crystal Polymers*; McArdle, C. B., Ed.; Chapman and Hall: New York, 1989.
(45) Shibaev, V. P.; Platé, N. A. *Adv. Polym. Sci.* **1984**, *60/61*, 173−252.
(46) Percec, V.; Hahn, B.; Ebert, M.; Wendorff, J. H. *Macromolecules* **1990**, *23*, 2092−2095.
(47) Kosaka, Y.; Uryu, T. *Macromolecules* **1995**, *28*, 8295−8301.
(48) Imrie, C. T.; Attard, G. S.; Karasz, F. E. *Macromolecules* **1996**, *29*, 1031−1035.
(49) Zhao, Y. F.; Yi, Y.; Fan, X. H.; Chen, X. F.; Wan, X. H.; Zhou, Q. F. *J. Polym. Sci., Part A* **2005**, *43*, 2666−2674.
(50) Tang, H.; Zhu, Z. G.; Wan, X. H.; Chen, X. F.; Zhou, Q. F. *Macromolecules* **2006**, *39*, 6887−6897.
(51) Yu, Z. N.; Wan, X. H.; Zhang, H.; Chen, X. F.; Zhou, Q. F. *Chem. Commun.* **2003**, 974−975.
(52) Farina, M. In *Topics in Stereochemistry*; Wiley-Interscience: New York, 1987; Vol. 17, pp 1−111.
(53) Green, M. M.; Cheon, K.-S.; Yang, S.-Y.; Park, J.-W.; Swansburg, S.; Liu, W. *Acc. Chem. Res.* **2001**, *34*, 672−680.
(54) Cornelissen, J. J. L. M.; Fischer, M.; Sommerdijk, N. A. J. M.; Nolte, R. J. M. *Science* **1998**, *280*, 1427−1430.
(55) Zhang, J.; Cao, H. Q.; Wan, X. H.; Zhou, Q. F. *Langmuir* **2006**, *22*, 6587−6592.
(56) Kelen, T.; Tüdos, F. *J. Macromol. Sci. Chem.* **1975**, *A9*, 1−27.
(57) Elias, H. G. *Macromolecules*; Plenum: New York, 1977; Vol. 2; Chapter 22, p 771.
(58) Gopalan, P.; Ober, C. K. *Macromolecules* **2001**, *34*, 5120−5124.
(59) Wintermantel, M.; Fischer, K.; Gerle, M.; Ries, R.; Schmidt, M.; Kajiwara, K.; Urakawa, H.; Wdtaoka, I. *Angew. Chem., Int. Ed.* **1995**, *34*, 1472−1474.

(60) Nakano, T.; Okamoto, Y.; Hatada, K. *J. Am. Chem. Soc.* **1992**, *114*, 1318−1329.
(61) The preliminary results were presented in the supporting information of ref 46. The samples used in the present work were newly synthesized and characterized by both GPC and GPS-LS. The absolute molecular weights of the polymers were thus obtained.
(62) Bailey, W. J.; Yates, E. T. *J. Org. Chem.* **1960**, *25*, 1800−1804.
(63) Pino, P.; Lorenzi, G. P. *J. Am. Chem. Soc.* **1960**, *82*, 4745−4747.
(64) Pino, P. *Adv. Polym. Sci.* **1965**, *4*, 393−456.
(65) Nomura, R.; Nakako, H.; Masuda, T. *J. Mol. Catal. A: Chem.* **2002**, *190*, 197−205.
(66) Flory, P. J. *Proc. R. Soc. London* **1956**, *A234*, 73−89.
(67) Wunderlich, B. *Macromolecular Physics*; Academic Press: New York, 1973, Vol. I.
(68) Green, M. M.; Park, J.-W.; Sato, T.; Teramoto, A.; Lifson, S.; Selinger, R. L. B.; Selinger, J. V. *Angew. Chem., Int. Ed.* **1999**, *38*, 3138−3154.

MA071141P